Materials Research. 2013; 16(6): 1411-1417
DOI: 10.1590/S1516-14392013005000138

Development and Comparison of n^+pn^+ and n^+pp^+ Solar Cells in Multicrystalline Silicon

Gabriela Wehr*[a], *Izete Zanesco*[b], *Adriano Moehlecke*[b]

[a]*Faculty of Mathematics, Pontifical Catholic University of Rio Grande do Sul – PUCRS, Av. Ipiranga, 6681, P.30, Bloco C, CEP 90619-900, Porto Alegre, RS, Brazil*
[b]*Faculty of Physics, Pontifical Catholic University of Rio Grande do Sul – PUCRS, Av. Ipiranga, 6681, P. 96A, TECNOPUC, CEP 90619-900, Porto Alegre, RS, Brazil*

Received: March 27, 2013; Revised: July 16, 2013

The goal of this paper is to present the development and comparison of p-type multicrystalline silicon solar cells with screen printed metallization. Industrial processes were developed to manufacture the $n^+pn^+$and n^+pp^+ solar cells. The n^+pn^+ structure was obtained with single phosphorus diffusion. The n^+pp^+ solar cell was developed and the p^+ region was optimized experimentally by using one single high temperature step for phosphorus and aluminum diffusion. The results showed that the average efficiency of n^+pn^+ solar cells with no texturing was 12.3%. The efficiency increased 1.5% (absolute) with the implementation of acidic solution texturing. The highest efficiency achieved for solar cell without (n^+pn^+) and with (n^+pp^+) back surface field (BSF) was 13.8% and 14.1%, respectively. The BSF does not result in a significant improvement in the efficiency when the diffusion is carried out in a single step thermal diffusion in industrial process with screen printed metallization.

Keywords: *solar cells, multicrystalline silicon, fabrication processes*

1. Introduction

Solar cells are devices that convert solar energy directly into electric energy. The conversion does not generate residue nor does it emit gas or noise. The photovoltaic (PV) market is dominated by PV modules manufactured with crystalline silicon wafers. In 2010, the production of solar cells had its highest increase (118%) in relation to the 2009 PV market[1]. In 2011, the production reached the 37 GW mark after a 36% increase[1]. This power output is 2.5 times greater than the output of the Itaipu hydroelectric power plant, the largest in Brazil. Crystalline silicon solar cells make up 88% of the market, out of which 57% are multicrystalline silicon cells (Si-Mc)[1]. The biggest world supplier is China. The country holds 57% of the solar cell world market.

The demand for multicrystalline silicon wafers has been on the rise due to increasingly low-cost crystallization processes, and to increasingly efficient solar cells. The rising demand for this type of device is a result of the improvement in the quality of the material. Ingot manufacture techniques and the evolution of manufacturing processes have boosted these improvements.

Multicrystalline silicon wafers are square-shaped and thus offer optimal use of the area of the photovoltaic module. The crystal growth method of multicrystalline silicon is simpler than the methods used to produce float-zone silicon (Si-FZ) or Czochralski silicon (Si-Cz). But the method used to obtain multicrystalline silicon inevitably results in the formation of grain boundaries and dislocations[2]. Consequently, the quality of the material is poorer than that of Si-FZ and Si-Cz substrates.

*e-mail: moehleck@pucrs.br

The main structures of crystalline silicon solar cells fabricated by the industry are n^+pp^+ and n^+pn^+. The latter are processed with single phosphorus diffusion. The back surface field (BSF) in the n^+pp^+ structure, in turn, is implemented by introducing a thermal step to diffuse the aluminum, which is usually deposited by screen printing. The screen printing technique is also used to deposit the front metal grid on the phosphorus emitter doped by $POCl_3$. The diffusion of dopants and the screen printed metallization in the rear face of the n^+pn^+ solar cells (without BSF) are produced with fewer steps. Moreover, an alternative to deposition of Al paste on the whole area of the rear side of the wafer is the deposition of a Al/Ag grid on the rear side. Consequently, in n^+pn^+ solar cells there is a reduction in the amount of metal paste used and in surface recombination. Nevertheless, the BSF solar cells are more efficient than n^+pn^+ solar cells.

The BSF solar cell fabricated with the typical industrial screen printed metallization and using 239 cm^2 Si-Cz wafers showed the efficiency (η) of 18.3%[3]. The average efficiency of Si-Cz solar cells in industrial manufacturing process is 16.5%[4]. Magnetic Czochralski-silicon (Si-MCz) has been used to develop 4 cm^2 solar cells that show 24.7% efficiency by using a laboratory process[5]. The best silicon solar cell was denominated PERL (passivated emitter and rear locally-diffused cell) and showed 25% efficiency[6]. The 4 cm^2 device was developed using Si-FZ selective emitter on the front face, and the locally-diffused boron on the backside. Both highly doped regions were manufactured using masks and photolitography processes.

The highest efficiency obtained with multicrystalline silicon cells was 20.4% for 1 cm^2 area. This solar cell was

processed with laser-fired rear contacts and with plasma textured front surface. Wet oxidation at low temperature (800 °C) was performed for rear surface passivation and maintenance of the high minority carrier lifetime. The 120 Ω/□ phosphorus emitter was contacted with a metal grid of Ti/Pd/Ag. In the front face, a thin thermal oxide was grown and a double-layer anti-reflection coating of TiO_2/MgF_2 was deposited[7]. Mitsubishi[8] achieved an efficiency of 19.3% for 217.7 cm^2 Si-Mc solar cell manufactured with the honeycomb structure texture. The texture combines laser-patterning and wet chemical etching. The screen-printed metallization and phosphorus diffusion were optimized in order to achieve this efficiency[9]. The company Q-Cells, in turn, reached the 19.5% efficiency in 242 cm^2 solar cells with laser-fired contacts and double-side passivation[5]. A standard isotropic inline-texturing process was used. Fine lines with a width of ~75 µm were screen-printed on the lowly doped emitter and thickened in a silver solution by light-induced plating[10]. Despite these improvements, the average industrial efficiency for Si-Mc solar cells is 15.5%, ranging from 14.5% to 16.2%[4].

One of the goals of solar cells research and development is to achieve more cost-effective manufacturing processes and produce more efficient solar cells. The aim of this paper is to present the development and comparison of n^+pn^+ and n^+pp^+ solar cells processed in p-type multicrystalline silicon wafers with screen printed metallization. The n^+pn^+ solar cells were developed with phosphorus diffusion in both sides. Metallization on the backside perforated the n^+ region to reach the base. The back surface field was not formed in these devices. To obtain BSF solar cells, that is, with the n^+pp^+ structure, the Al p^+ region (Al-BSF) had to be experimentally optimized. To develop a cost-effective manufacturing process, the Al-BSF was formed during the thermal step for phosphorus diffusion

2. Material and Methods

Two complete solar cell manufacturing processes were optimized by using 60 mm × 60 mm samples obtained from 125 mm × 125 mm, p-type, 0.5 to 2 Ω.cm and 240 µm thick multicrystalline silicon wafers.

The manufacturing process for n^+pn^+ multicrystalline silicon solar cells (without BSF) was implemented as follows: RCA cleaning, phosphorus diffusion based on $POCl_3$ in a conventional quartz tube furnace, phosphorus silicate glass (PSG) removal and RCA cleaning, TiO_2 anti-reflection coating (ARC) deposition by the electron beam technique, screen printed metallization and laser edge isolation[11]. The RCA cleaning was performed using analytic grade chemicals and deionized water with electric resistivity above 18 MΩ.cm. A metal grid with two busbars was deposited on the front and rear face. The areas covered by Ag paste (front face) and Ag/Al paste (rear face) were 8% and 53%, respectively. The metal coverage on the rear face was optimized by solar cell simulation. The complete process included the solar cell surface texturing. The manufacturing process is illustrated in Figure 1.

Aluminum deposition by e-beam evaporation was introduced to the BSF solar cell (n^+pp^+) manufacturing process. The single step diffusion of phosphorus and aluminum was developed using a conventional quartz tube furnace. This process was based on results obtained in Si-Cz wafers[12].

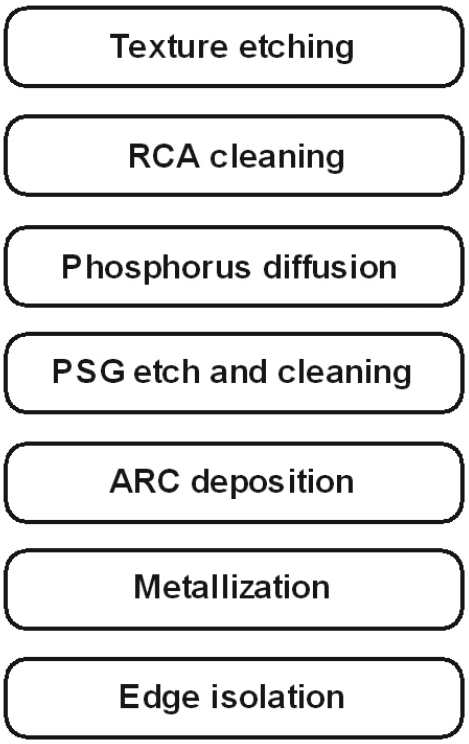

Figure 1. n^+pn^+ silicon solar cell manufacturing process.

Silicon oxide growth is required to form the BSF in the manufacture of solar cells with diffusion of aluminum deposited by evaporation. Photoresist is deposited on one surface and silicon oxide removal is performed on the other surface. Thus, phosphorus diffusion occurs only in the front face. Following the oxide etching in chemical solution, the aluminum on the back surface is evaporated and diffused[11,13].

A manufacturing process was developed to obtain n^+pp^+ Si-Mc solar cell and avoid oxidation, deposition of photoresist, and silicon oxide etching. The process was carried out with single-step thermal diffusion of phosphorus and aluminum. As a result, the production cost was reduced. The process incorporated the following steps (see Figure 2): surface texturing using acidic solution, RCA cleaning, Al evaporation, single step Al and P diffusion, phosphorus silicate glass removal, RCA cleaning, TiO_2 anti-reflection coating deposition, screen printed metallization, firing of metallization pastes, and laser edge isolation.

The thickness of evaporated aluminum in n^+pp^+ solar cells was 2 µm and the thickness of TiO_2 anti-reflection coating was 68 nm. The Ag paste covered an area of 9% on the front face. The metallization paste firing was implemented using a belt furnace, with temperature set at 870 °C and belt speed at 190 cm/min.

After the solar cells were processed, they were evaluated by measuring the electric current density versus applied voltage (J-V) characteristic. Measurements were carried

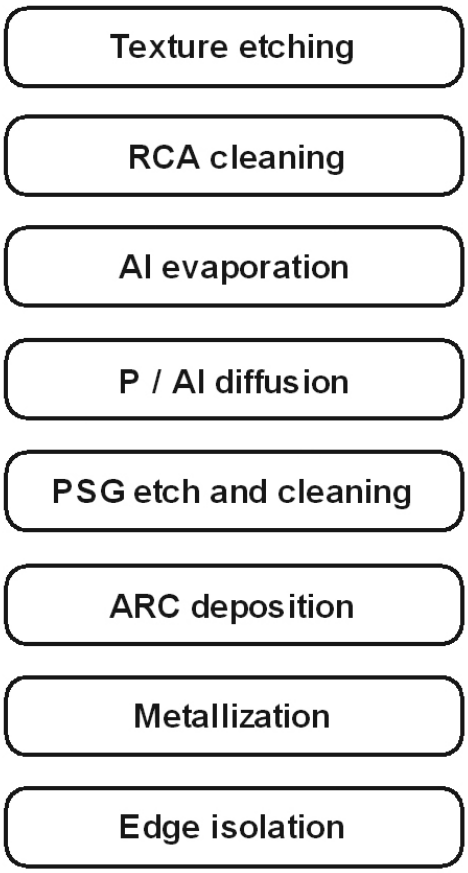

Figure 2. n^+pp^+ silicon solar cell manufacturing process.

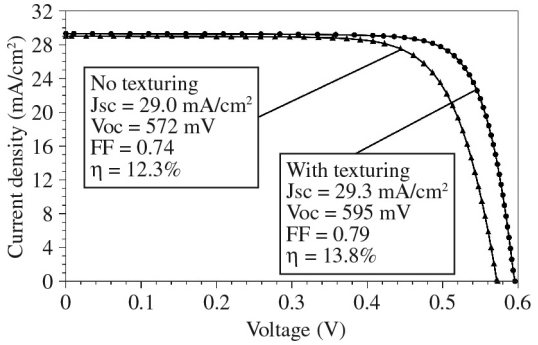

Figure 3. Electrical characteristics at standard conditions of the n^+pn^+ solar cells with and without texturing etching in acidic solution.

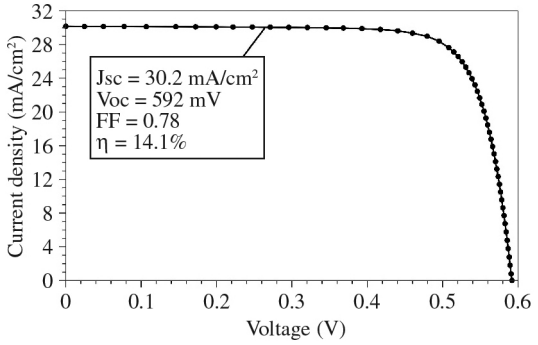

Figure 4. Electrical characteristic of the n^+pp^+ solar cell at standard conditions.

out following the international standard: irradiance of 1000 W/m^2 with spectrum AM 1.5G and cell temperature of 25 °C. The standard solar cell was calibrated at the *Fraunhofer Institut für Solare Energiesysteme*, Germany. The solar cells were also characterized by minority carrier diffusion length and quantum efficiency. Experimental results were also analyzed by simulating solar cells using the PC-1D software.

3. Results and Discussion

3.1. *n^+pn^+ solar cells with and without texturing*

The manufacturing process for solar cells without BSF and no texturing lead to an efficiency of 12.3%. The cell presented the short-circuit density (J_{SC}) of 29 mA/cm^2, open circuit voltage (V_{OC}) of 572 mV and fill factor (FF) of 0.74. These results were achieved with phosphorus diffusion at 875 °C, which resulted in the 30 Ω/□ sheet resistance. The temperature of 860 °C was used for metallization paste firing.

Figure 3 shows the comparison between n^+pn^+ solar cell J-V curves with and without surface texturing. If the process included the texturing step, the maximum efficiency achieved was 13.8%, which is 1.5% (absolute) higher than the efficiency of the solar cell without texturing. The electrical parameters of the solar cell with texturing were: J_{SC} = 29.3 mA/cm^2, V_{OC} = 595 mV and FF = 0.79. Texturing etch increased the fill factor and V_{OC}, mainly. The positive results might have been obtained due to the improvement in the contact between metal and semiconductor. Texturing improved the J_{SC} slightly. The increase in J_{SC} was associated with the reduction of reflection in the front surface. The average reflectance was reduced from 35% to 23% with the implementation of the texturing etch. Following the deposition of TiO_2 anti-reflection coating, the average reflectance decreased to 6.4% for samples with texturing, and to 7.5% for samples without texturing etch. In this process, phosphorus diffusion was also carried out at 875 °C and the sheet resistance of approximately 35 Ω/□ was obtained. Metallization paste firing was performed at 870 °C.

3.2. *n^+pp^+ solar cells*

The experimental optimization of the manufacturing process of solar cells with BSF showed that the best result was obtained with diffusion of both dopants at 875 °C, and with aluminum diffusion for 90 minutes. The sheet resistance in the n^+ region was 64 Ω/□.

The efficiency for n^+pp^+ solar cells was 14.1%. Figure 4 shows the J-V characteristic obtained under standard measuring conditions. The parameters were J_{SC} = 30.2 mA/cm^2, V_{OC} = 592 mV and FF = 0.78.

3.3. *Comparison of solar cells with and without BSF*

3.3.1. Analysis of electrical parameters

The results for solar cells with texturing showed that the BSF region did not significantly improve the efficiency. The device with BSF reached the efficiency of 14.1% and the solar cell with the single phosphorus diffusion, in turn, achieved the efficiency of 13.8%. The J_{SC} was the parameter that increased with aluminum diffusion. The software PC-1D was used to simulate solar cells, starting from the parameters presented in Table 1. The thickness of Si wafers was varied to evaluate solar cells with and without BSF. The reflectance of the TiO_2 anti-reflection coating was considered in the simulation. The solar cells without BSF were simulated using n^+p structure because the rear metal grid perforated the n^+ region. The simulated results are presented in the Table 2.

The 240 μm thick Si-Mc solar cell showed a 1.4% (absolute) increase in efficiency for the device with BSF in comparison with the solar cell without BSF. This thickness is similar to that of the solar cells developed and the improvement in the efficiency is higher than the value of 0.3% (absolute) obtained with the manufactured solar cells. For the devices with BSF, the main difference between experimental and simulated results was in V_{OC}. This result, in combination with a slight difference in the fill factor, was associated with the low experimental efficiency. The difference between experimental and simulated efficiency may be related to the single step diffusion for the two dopants (which may affect the effectiveness of BSF), the different base resistivity or the inferior quality of the Si-Mc substrate. Moreover, the Ag/Al paste used to make the rear grid, which covers 53% of the area, may be causing BSF in n^+pn^+ solar cells.

The experimental efficiency of the n^+pn^+ solar cell was similar to that obtained by simulation. However, the experimental result presented higher J_{SC} and lower V_{OC} than the simulated values. The electric current density was higher because the Al/Ag paste may be causing BSF. The voltage was lower due to grain boundaries and dislocations in the Si-Mc material. The simulated and experimental FF values were similar for both kinds of solar cells. This result confirms that metal grids were formed in near optimal conditions.

The BSF solar cell efficiency was modestly affected by the reduction of the thickness from 400 μm to 100 μm. The V_{OC} increased slightly, and the J_{SC} decreased. However, for devices without BSF, the efficiency decreased as function of the reduction in thickness. In these cells, J_{SC} decreased. Thus the result is similar to the result for the cells with BSF, though there was a decrease in V_{OC}.

3.3.2. Analysis of minority carrier diffusion length and quantum efficiency

The minority carrier diffusion length (L_D) of the n^+pn^+ and n^+pp^+ solar cells was also compared, as shown in Figure 5. The result was obtained from the light beam induced current (LBIC) measurements carried out with WT1000-PV equipment (Semilab). The average diffusion length for 132 μm BSF solar cells was 20% greater than the average value measured in the solar cells without BSF (L_D = 112 μm). This result indicates the low effectiveness of the BSF. For both types of solar cells, the L_D was inferior to the thickness of the cell of 240 μm. In this case, the BSF had little effect on the dark saturation current. If the minority carrier lifetime is high (i.e., the minority carrier diffusion length is greater than the thickness of the solar cell), the minority carriers reach the BSF easily and the dark saturation current becomes a function of the rear recombination velocity[2].

The external quantum efficiency (EQE) of three solar cells was also measured: Cel-PT3 with η = 14.0%, Cel-PT10 with η = 9.2% (both with BSF) and Cel-NT21 with η = 13.1% (without BSF). The comparison of the two-dimensional distribution of the EQE obtained with a laser radiation wavelength of 973 nm is shown in Figure 6.

The average EQEs of the solar cells Cel-PT3, Cel-PT10 and Cel-NT21 were 54.4%, 55.8% and 51.5%, respectively. The BSF did not significantly affect the EQE. The solar cells Cel-PT3 and Cel-PT10 showed only slightly higher EQE values when compared with cell Cel-NT21 (without Al-BSF). This result confirms the low effectiveness of the BSF obtained with the single thermal step for the diffusion of phosphorus and aluminum. The J-V curve shows that the solar cell Cel-PT10 had a high series resistance. The resistance has a negative effect on the fill factor and, consequently, reduces the $V_{OC,}$ as shown in Figure 7. This finding may be related to the formation of aluminum oxide (Al_2O_3) during the diffusion of phosphorus, which, in turn, damages the formation of the metal-semiconductor contact on the rear face.

Table 1. Parameters for simulation of n^+pn^+ and n^+pp^+ solar cells.

Parameters	Value
Bulk resistivity	1 Ω.cm
Minority carrier lifetime	60 μs
Average reflectance	6.4%
Phosphorus surface concentration	1×10^{20} cm^{-3}
Junction depth	0.5 μm
Al-BSF depth	3 μm
Front surface recombination velocity	1×10^4 cm/s
Back surface recombination velocity	1×10^7 cm/s

Table 2. Electrical parameters of the solar cells simulated as a function of thickness of the silicon multicrystalline wafer.

	Thickness (μm)	J_{SC} (mA/cm^2)	V_{OC} (mV)	FF	η (%)
n^+pn^+ (without BSF)	100	26.4	597.6	0.79	12.5
	200	27.9	614.1	0.79	13.6
	240	28.3	617.8	0.79	13.9
	400	29.0	626.1	0.79	14.4
n^+pp^+ (BSF)	100	29.5	644.0	0.80	15.1
	200	30.0	640.1	0.80	15.3
	240	30.0	638.9	0.80	15.3
	400	30.0	635.7	0.79	15.2

3.3.3. Analysis of the influence of base resistivity

Base resistivity is a parameter that influences the performance of solar cells with and without BSF in different ways. The substrate used in this study had a resistivity between 0.5-2.0 Ω.cm. In low resistivity materials (<1 Ω.cm), BSF has less effect in the efficiency of the solar cell. BSF is recommended for substrates with greater resistivity. It is also recommended if the wafer thickness is lower than the minority carrier diffusion length.

The solar cell simulations were carried out using a thickness of 240 μm and the parameters in Table 1. The base resistivity was varied according to the figures in Table 3. Both kinds of solar cells showed an increase in efficiency with the reduction of base resistivity. If the resistivity is increased from 0.5 to 2 Ω.cm, the solar cells without BSF

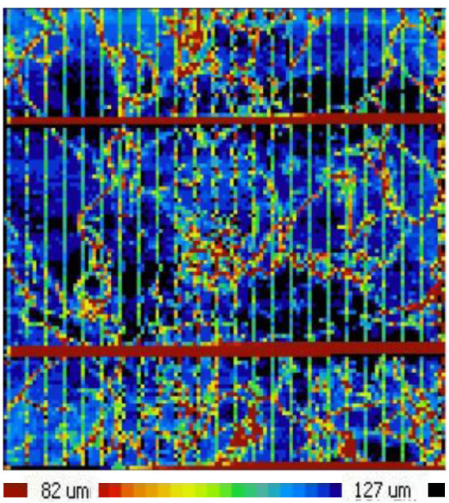

(a)

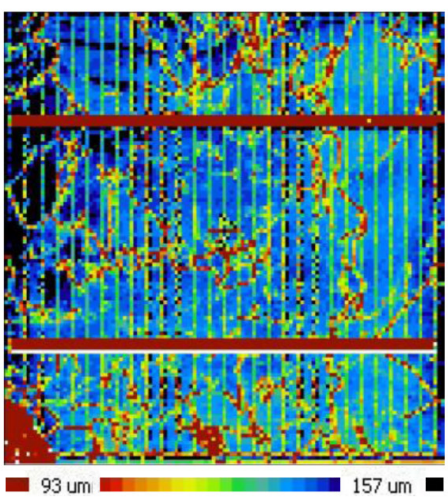

(b)

Figure 5. Two-dimensional distribution of the minority carrier diffusion length in (a) n⁺pn⁺ and (b) n⁺pp⁺ solar cells.

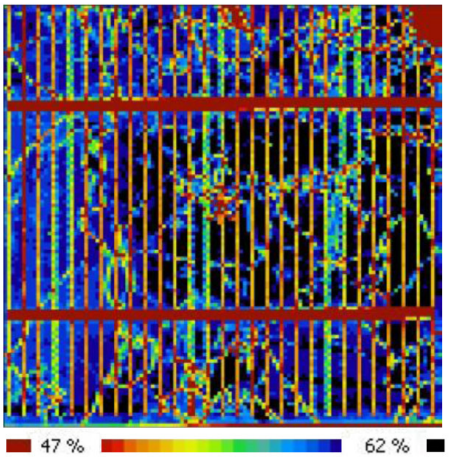

(a)

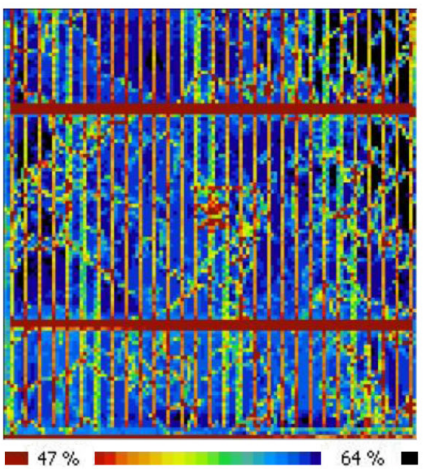

(b)

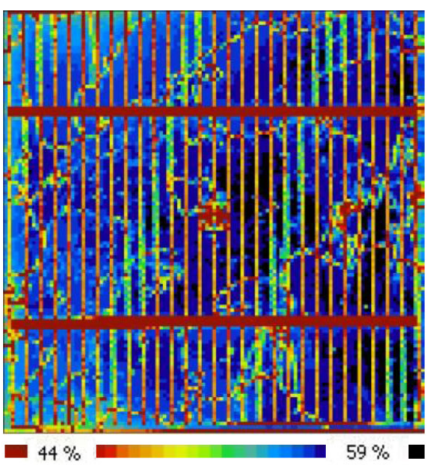

(c)

Figure 6. Two-dimensional distribution of the EQE of the solar cells (a) Cel-PT3 (n⁺pp⁺), (b) Cel-PT10 (n⁺pp⁺) and c) Cel-NT21 (n⁺pn⁺).

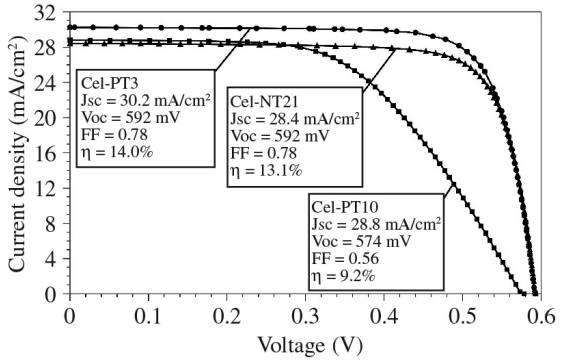

Figure 7. Current density as a function of the voltage of the solar cells Cel-PT03 (n^+pp^+), Cel-PT10 (n^+pp^+) and Cel-NT21 (n^+pn^+).

Table 3. Electrical parameters for n^+pn^+ and n^+pp^+ solar cells with 240 µm thickness as a function of the base resistivity of the Si-Mc substrate.

	Resistivity (Ω.cm)	J_{SC} (mA/cm²)	V_{OC} (mV)	FF	η (%)
n^+pn^+	0.5	28.2	636.8	0.80	14.4
	1	28.3	617.8	0.79	13.9
	2	28.3	597.9	0.79	13.3
	10	28.5	551.7	0.77	12.1
n^+pp^+	0.5	29.6	648.8	0.80	15.3
	1	30.0	638.9	0.80	15.3
	2	30.3	627.8	0.79	15.0
	10	30.5	604.1	0.76	14.1

showed a reduction of 1.1% (absolute) in efficiency. This result is superior to the 0.3% reduction for solar cells with BSF. There was a slight decrease in J_{SC} with the reduction in the base resistivity. However, the fill factor and V_{OC} increased for both solar cells.

The base resistivity of 10 Ω.cm resulted in the efficiency of 14.1%, which is equivalent to the experimental result for BSF devices (see Table 3). Base resistivity explains also the difference between experimental results of solar cells with and without BSF. The V_{OC} of 604 mV obtained in the simulation was the closest value to the experimental value of 592 mV.

4. Conclusions

The n^+pn^+ solar cells with no texturing reached the maximum efficiency of 12.3%. The solar cells with texturing, in turn, achieved the efficiency of 13.8%, thus 1.5% (absolute) higher than that of solar cells without texturing. In solar cells with texturing, the main increase occurred in the fill factor and the open circuit voltage. The efficiency of solar cells with BSF and texturing was 14.1%. In this case, the J_{SC} increased when compared with the value found in solar cells without BSF. The simulation of solar cells showed that the BSF may enhance efficiency up to 1.4%. Finally, the V_{OC} parameter presented the biggest difference between experimental and simulated values.

For solar cells without BSF, the experimental efficiency was similar to the simulated efficiency, but there were differences in V_{OC} and J_{SC}. The fill factor presented similar experimental and simulated results for both kinds of solar cells. The reduction in the thickness of the substrate caused a modest reduction in the efficiency of BSF solar cells, however affected the solar cells without BSF more significantly.

The minority carrier diffusion length was only 20% higher for BSF cells. This result shows that the single step thermal diffusion of phosphorus and aluminum produces a less-effective BSF. The efficiency of some BSF solar cells was limited by series resistance. This series resistance possibly results from the formation of aluminum oxide (Al_2O_3) during the diffusion of phosphorus. Consequently, the back metal-semiconductor contact may be affected.

Simulations showed that the efficiency of solar cells with and without BSF increases with the reduction of base resistivity. The efficiency of the simulated BSF solar cells with 10 Ω.cm base resistivity was equivalent to the experimental result.

In conclusion, base resistivity may be associated with the fact that there was a small difference of 0.3% (absolute) between the efficiency of devices with and without BSF. Another factor that influenced the result was the low effectiveness of the BSF formed during single step phosphorus and aluminum diffusion.

Acknowledgments

The authors gratefully acknowledge the financial support of the State Electric Energy Distribution Company (CEEE-D), contract CEEE/D2009-9928171.

References

1. Hering G. Enter the dragon. *Photon International.* 2012:132-160.
2. Luque A and Hegedus S. *Handbook of Photovoltaic Science and Engineering*. West Sussex: John Wiley&Sons; 2003. 1115 p. http://dx.doi.org/10.1002/0470014008
3. Ebong A, Cooper IB, Rounsaville A, Rohatgi A, Borland W, Mikeska K et al. Overcoming the technological challenges of contacting homogeneous high sheet resistance emitters (HHSE). In: *Proceedings of the 26th European Photovoltaic Solar Energy Conference and Exhibition*; 2011; Hamburg, Germany. WIP; 2011. p. 1747-1749.
4. Fath P, Keller S, Winter P, Joss W and Herbst W. Status and perspective of crystalline silicon solar cell production. In: *Proceedings of the 34th IEEE Photovoltaic Specialists Conference (PVSC)*; 2009; Philadelphia, USA. IEEE; 2009. p. 2471-2476. http://dx.doi.org/10.1109/PVSC.2009.5411274
5. Green MA, Emery K, Hishikawa Y, Warta W and Dunlop Ewan D. Solar cell efficiency tables (Version 41). *Progress in Photovoltaics*: Research and Applications. 2013; 21:1-11. http://dx.doi.org/10.1002/pip.2352
6. Green MA, Zhao J, Wang A and Wenham SR. Very high efficiency silicon solar cells – science and technology. *IEEE Transactions on Electron Devices*. 1999; 46(10):1940-1947. http://dx.doi.org/10.1109/16.791982

7. Schultz O, Glunz SW and Willeke GP. Multicrystalline silicon solar cells exceeding 20% efficiency. *Progress in Photovoltaics*: Research and Applications. 2004; 12:553-558 http://dx.doi.org/10.1002/pip.583

8. Green MA, Emery K, Hishikawa Y and Warta W. Solar cell efficiency tables (version 37). *Progress in Photovoltaics*: Research and Applications. 2011; 19:84-92. http://dx.doi.org/10.1002/pip.1088

9. Niinobe D, Nishimura K, Matsuno S, Fujioka H, Katsura T, Okamoto T et al. Honeycomb structured multi-crystalline silicon solar cells with 18.6% efficiency via industrially applicable laser-process. In: *Proceedings of the 23rd European Photovoltaic Solar Energy Conference and Exhibition*; 2008; Valencia, Spain. WIP; 2008. p. 1824-1828.

10. Engelhart P, Zimmermann G, Klenke C, Wendt J, Kaden T, Junghänel M et al. R&D pilot-line production of multi-crystalline Si solar cells with top efficiencies exceeding 19%. In: *Proceedings of the 37th IEEE Photovoltaic Specialists Conference (PVSC)*; 2011; Seattle, USA. IEEE; 2011. p. 1919-1923.

11. Moehlecke A and Zanesco I. Development of silicon solar cells and photovoltaic modules in Brazil: analysis of a pilot production. *Materials Research,* 2012; 15:581-588. http://dx.doi.org/10.1590/S1516-14392012005000084

12. Zanesco I and Moehlecke A. *Implementação de duas unidades geradoras de energia elétrica com módulos fotovoltaicos eficientes*. Porto Alegre; 2010. 387 p. Relatório técnico, MME 008/2005.

13. Moehlecke A and Zanesco I. Pilot production of n^+pn^+ and n^+pp^+ silicon solar cells: efficiency x yield. In: *Proceedings of the 25th European Photovoltaic Solar Energy Conference and Exhibition and 5th World Conference on Photovoltaic Energy Conversion*; 2010; Valencia, Spain. WIP; 2010. p. 2497-2500.